JOURNAL OF APPLIED POLYMER SCIENCE VOL. 21 2341–2358 (1977)

Melt Spinning of Nylon 6: Structure Development and Mechanical Properties of As-Spun Filaments

VILAS G. BANKAR, JOSEPH E. SPRUIELL, and JAMES L. WHITE,
Department of Chemical and Metallurgical Engineering, The University of Tennessee, Knoxville, Tennessee 37916

Synopsis

The structure of melt-spun nylon 6 filaments was studied using on-line x-ray diffraction and birefringence measurements. Measurements were also made on as-spun and treated filaments. On-line wide-angle x-ray scattering measurements indicated that crystallization did not occur on the nylon 6 spinline at spinning rates up to 1000 m/min when spinning was done into either ambient air of 60% relative humidity or into wet saturated air. The filaments did crystallize gradually on the bobbin to a paracrystalline pseudohexagonal (γ) form. The rate of crystallization was dependent on the molecular orientation developed in the spun filaments. Crystalline orientation factors based on hexagonal symmetry were computed as a function of take-up velocity for fibers which were conditioned 24 hr in air at 65% relative humidity. Annealing in air or treatment in water or 20% formic acid solution causes a transformation from the pseudohexagonal form to the α monoclinic form. The tangent modulus of elasticity and tensile strength of spun and conditioned filaments increase with increasing take-up velocity and spinline stress, while elongation to break decreases with these variables.

INTRODUCTION

Nylon 6 is one of the most important of commercial synthetic fibers.[1] While originally synthesized by Carothers and Berchet[2] and studied by du Pont[2,3] about 1930 as part of their pioneering development of melt spinning, nylon 6 was not successfully developed until the end of the decade by I. G. Farbenindustrie.[1,4] In this paper, we will present a study of structure development during the melt spinning of nylon 6 fiber, structural changes occurring in posttreatments of melt-spun fibers, and mechanical properties of these fibers.

The crystalline structure of nylon 6 was first investigated by Brill[5] who found the unit cell of drawn fibers to be monoclinic in character and determined the cell dimensions. The problem was later reinvestigated by Holmes, Bunn, and Smith[6] who confirmed Brill's results and gave improved values for the unit cell dimensions and angles. These authors also pointed to the existence of small amounts of a second crystallographic form in drawn nylon 6 fibers. This point was subsequently investigated by later researchers.[7–11] Wide-angle x-ray (WAXS) patterns of quenched nylon 6 film were made by Sandeman and Keller[12] who noted that their results were very different from those of Holmes et al. Ziabicki and Kedzierska[13] studied melt-spun (but undrawn) nylon 6 filament.

© 1977 by John Wiley & Sons, Inc.

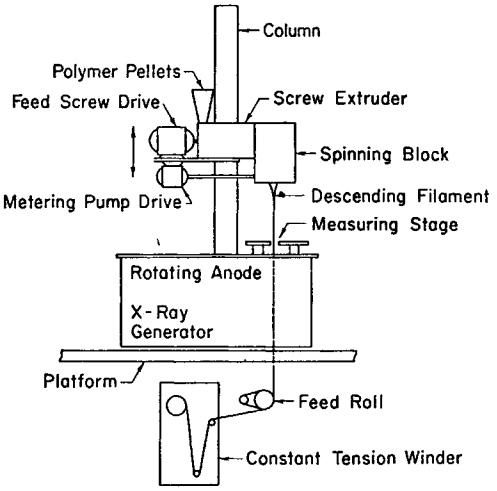

Fig. 1. Melt spinning apparatus.

They found a similar poorly formed crystalline structure represented by a broad equatorial reflection corresponding to an interplanar spacing of 4.2 Å and a meridional reflection at 8.3 Å. Cold drawing or hot-water treatment yielded the Holmes-Bunn-Smith monoclinic structure, which is generally referred to as the α form. The crystalline form of melt-spun fibers was subsequently identified by Vogelsong[10] as being the same as the second phase observed in drawn fibers. Roldan and Kaufman[14] and later Parker and Lindenmeyer[15] have attempted to rationalize all of these observations. The former authors distinguish between various classifications of amorphous, monoclinic α (Holmes et al.), paracrystalline monoclinic (Brill), hexagonal β, and a nematic pseudohexagonal γ (Ziabicki-Kedzierska).

As mentioned above, the basic studies of structure development during the melt spinning of nylon 6 are due to Ziabicki and Kedzierska[13,16] who studied both WAXS patterns and birefringence of spun fibers. The birefringence Δn was correlated as an increasing function of spinline stress. More recently, Hamana, Matsui, and Kato[17] and Ishibashi, Aoki, and Ishii[18] have made on-line measurements of birefringence and determined Δn as a function of spinline position. Ishibashi et al. note that undrawn yarns exhibit increases in birefringence if placed in a 50% relative humidity environment. Ishibashi and Ishii[19] have also investigated the effect of heating chambers placed around the spinline on the birefringence of the running filament. They have suggested that the increased birefringence observed is due to crystallization of the running filament. Further studies of melt-spun nylon 6 fibers are reported by Pasika, West, and Thurston,[20] Sakaoku, Morosoff, and Peterlin,[21] and Wasiak and Ziabicki.[22] Considerations of the mechanical properties of melt-spun fibers as related to drawing have been published by Yumoto,[23,24] Hattori, Takagi, and Kawaguchi,[25,26] Sakaoku et al.,[21] and Kitao, Kobayoshi, Ikegami, and Ohya.[27,28] Structure development in the wet spinning of nylon 6 has been described by Kiyotosukuri, Hasegawa, and Imamura[29] and by Hancock, Spruiell, and White.[30] They found that in most cases the wet-spun fibers exhibited the α monoclinic form.

While there has been substantial research on structure development in melt spinning of nylon 6, many of the most basic questions remain unanswered. It

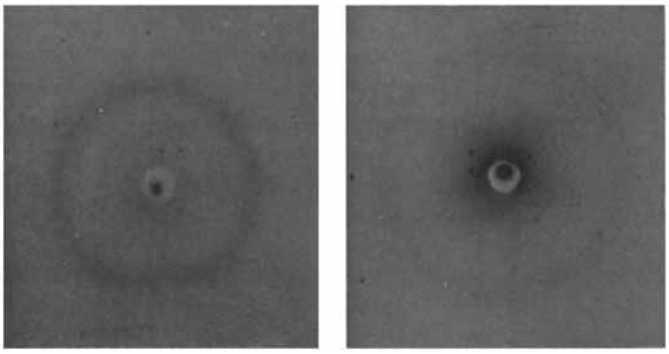

(a) (b)

Fig. 2. Typical WAXS patterns measured on-line for a nylon 6 spinline: (a) 100 m/min, take-up velocity 160 cm below the spinneret, T = 95°C, 60% relative humidity; (b) 556 m/min, take-up velocity 120 cm below the spinneret, T = 96°C, 100% relative humidity.

is not known under what conditions this polymer crystallizes in the spinline and when it crystallizes on the bobbin. There have been no quantitative studies of the relationship of the crystalline orientation of spun fibers with spinning conditions. In this paper, we turn our attention to these problems. We will examine a running threadline using on-line WAXS and birefringence measurements. On-line WAXS measurements were first carried out on a fiber spinline by Chappell, Culpin, Gosden, and Tranter[31] and later more quantitatively by Katayama, Amano, and Nakamura,[32] Dees and Spruiell,[33] and Henson and Spruiell[34] (see Spruiell and White[35]). Recently, Spruiell and White[36] have reviewed studies of structure development during melt spinning. This paper represents a continuation of research on this topic by the authors and their colleagues at the University of Tennessee.[33–38] It also represents a contribution to our ongoing studies of nylon 6.[30,39,40] In a recent paper, we have considered the dynamic and rheological aspects of melt spinning of nylon 6.[39]

EXPERIMENTAL

Material

Nylon 6 chips were supplied by the American Enka Company (Lowland, Tennessee). Before use for any experiments, the polymer was dried at a pressure of 0.5 in. of mercury at 110°C. The sample was held under these conditions for 16 hr and then allowed to cool for 4 hr. Under these conditions, the polymer had a number-average molecular weight of 22,500 and a ratio of weight-average to number-average molecular weight of 2.08 as measured in the American Enka laboratories. The moisture content was measured using a MEECO electrolytic moisture analyzer, Model W Type LBY. The moisture content of the dried sample was 0.03–0.04%. This is the same polymer considered in our earlier paper[39]

Melt Spinning

The melt spinning operation and the measurement of forces on the spinline were discussed in some detail in our earlier paper.[39] The spinning apparatus

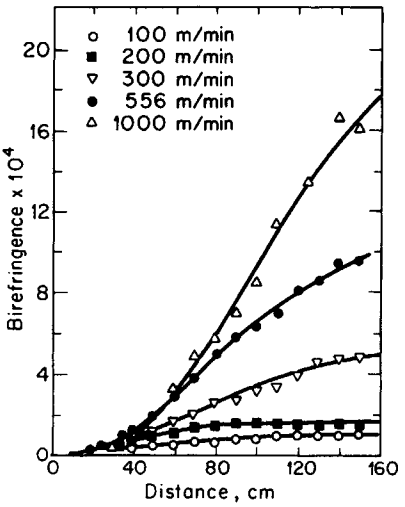

Fig. 3. On-line birefringence measurements show Δn as a function of position for several take-up velocities.

used is shown schematically in Figure 1. The fiber was melt spun through a Fourné screw extruder with a 1.3-cm-diameter screw. The extruder has a 7-liter N_2-purged hopper through which dry pellets were fed. The melt was fed from the screw through a Zenith metering pump to the spinneret block and extruded through a capillary of diameter 0.0762 cm and L/D ratio of 5. The fiber spinline was passed through a rotating-anode x-ray generator, presently to be discussed, and was taken up with a Leesona constant-tension winder. The entire extruder assembly was mounted on a vertical steel column; it could be moved up and down the column at will. Fiber diameters were measured by taking photographs, and temperatures were measured with a Hastings-Raydist null-balance contact thermocouple. These techniques and resulting diameter, velocity, and temperature profiles are discussed in our earlier paper.[39] More information is available in the Ph.D. dissertation of Bankar.[40]

Environmental Chamber

An environmental chamber in which the humidity could be controlled at any desired level surrounded a portion of the spinline. This enclosure was mounted between the spinneret and the rotating-anode generator. It consisted of a flexible canvas duct, 16 in. in diameter, connected at one end to the spinning block and at the other end to a wooden box with dimensions 18 × 17 × 22 in. Provisions were made to insert the x-ray collimator and film cassette into the box. The chamber was humidified with a nitrogen gas–steam mixture. The flow of steam was controlled by means of a Honeywell H93A humidity controller.

On-Line Structure Detection

WAXS. Wide angle x-ray diffraction patterns were made on-line using a Rigaku RU3V rotating anode x-ray generator. Nickel-filtered CuK_α radiation was used. Exposure times varied from 3 to 5 hours depending on the filament size.

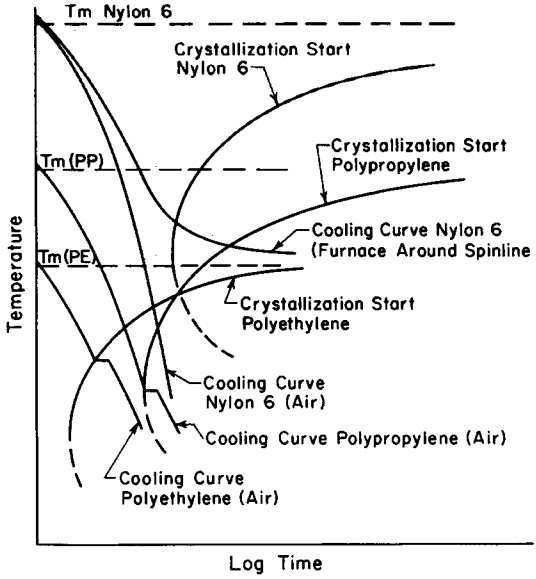

Fig. 4. Continuous cooling transformation diagram representation of structure development in nylon 6 and comparison with polyolefins.

On-Line Birefringence. The birefringence was determined using an Olympus polarizing microscope Model POS with a Berek compensator. The birefringence was computed by dividing the measured retardation by the fiber diameter. The microscope was placed on the x-ray table and the extruder was moved up and down so birefringence could be determined as a function of position along the spin path.

Characterization of Spun Filaments

SAXS. Small-angle x-ray diffraction (SAXS) patterns were determined using a Kiessig camera with pinhole collimation. The camera was mounted on the Rigaku rotating-anode x-ray generator; it was evacuated by a mechanical vacuum pump to reduce air scattering. An exposure time of 10 hr was used.

WAXS. This type of x-ray pattern was obtained using the same Kiessig camera but eliminating the extension tube used in the SAXS studies.

An XRD-5 General Electric x-ray diffractometer was also used to scan the x-rays scattered by the filaments. This instrument was used to determine Hermans-Stein-Wilchinsky[41–43] orientation factors for the pseudohexagonal unit cell of the melt-spun fiber. This approach to analysis of crystalline orientation of fibers as a function of spinning conditions was introduced by Kitao et al.[27,44] and by the Tennessee group.[33–38] The orientation factor for the j-crystallographic axis is

$$f_j = \frac{3\overline{\cos^2 \Phi_{j,z}} - 1}{2} \tag{1}$$

where $\Phi_{j,z}$ is the angle between the fiber axis and the j-crystallographic axis. Assuming rotational symmetry about the fiber axis,

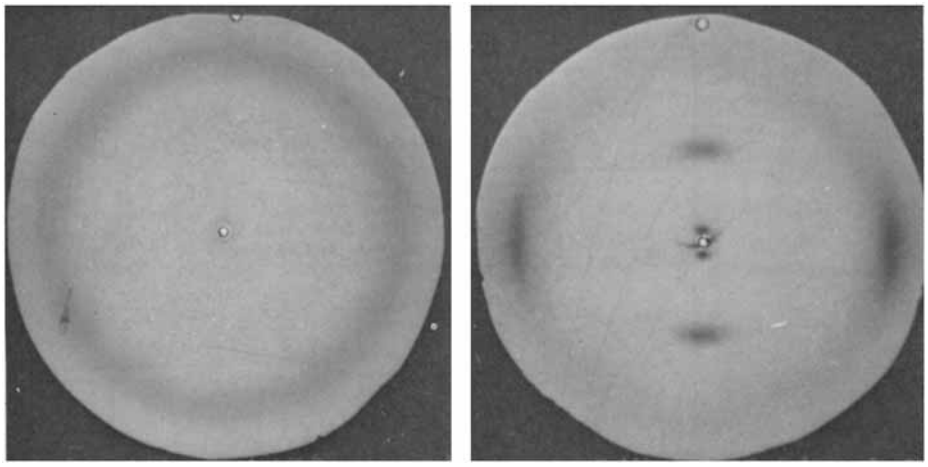

(a) (b)

Fig. 5. WAXS patterns for as-spun filaments taken in a vacuum camera immediately after spinning: (a) 200 m/min; (b) 1000 m/min.

$$\overline{\cos^2 \Phi_{j,z}} = \frac{\int_0^{\pi/2} I_{hkl}(\Phi_{j,z}) \cos^2 \Phi_{j,z} \sin \Phi_{j,z} d\Phi_{j,z}}{\int_0^{\pi/2} I_{hkl}(\Phi_{j,z}) \sin \Phi_{j,z} d\Phi_{j,z}} \tag{2}$$

where $I_{hkl}(\Phi_{j,z})$ represents the intensity diffracted from (hkl) planes which are normal to the j-crystallographic axis as a function of the azimuthal angle $\Phi_{j,z}$. For the pseudohexagonal unit cell of melt-spun nylon 6 filaments, there are no convenient reflections from planes perpendicular to either the a- or c-axis. The most suitable reflection for intensity measurements is the 100 corresponding to a d-spacing of 4.3 Å. Using intensity measurements for this reflection in eq. (2) allows computation of an orientation factor for a crystallographic direction, henceforth called a', which is normal to the (100) planes and also the c-axis. Using Wilchinsky's analysis,[43] it is readily shown that the c-axis orientation factor, f_c (chain axis), is given by $f_c = -2f_{a'}$.

Posttreatment of Spun Fibers

The as-spun fibers were subjected to various treatments and then retested using SAXS, WAXS, and birefringence measurements. The samples were (1) treated with water at 25°, 60°, and 100°C for 2 hr, (2) treated with a 20% formic acid solution at 25°, 75°, and 102°C for 2 hr, and (3) annealed in a vacuum oven at 70°, 100° and 150°C for 2 hr.

Mechanical Properties

A table model Instron tensile tester was used to obtain force elongation curves on the melt-spun fibers. The fibers were tested only after conditioning at 65% relative humidity and 20°C for 24 hr. The tests were carried out using initial fiber lengths of 1 in. and a cross-head speed of 1 in./min.

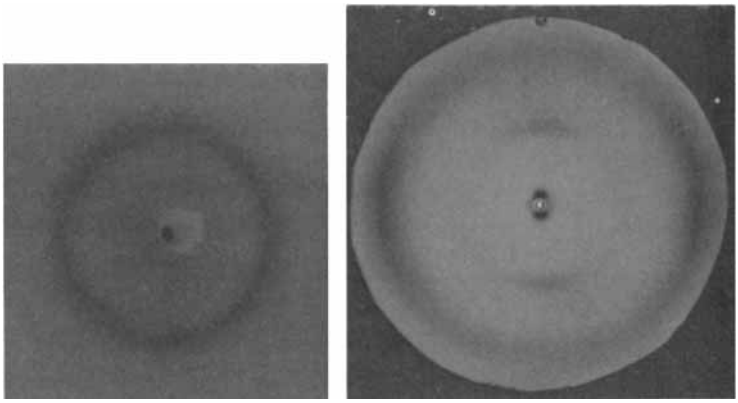

(a) (b)

Fig. 6. WAXS patterns of spun filaments conditioned for 24 hr at 65% relative humidity and 24°C: (a) 100 m/min; (b) 556 m/min.

ON-LINE STRUCTURE DEVELOPMENT

Results

Typical examples of on-line WAXS patterns are presented in Figure 2. In all cases, similar results were obtained whether spinning was carried out in air at 65% relative humidity or at 100% relative humidity. Also, there appeared to be little effect of take-up velocity in the range up to 1000 m/min which was investigated. As shown in Figure 2, a single diffuse halo was obtained in all cases. This corresponds to a Bragg's law d-spacing of 4.2 to 4.3 Å.

The birefringence Δn of the running filaments measured at various positions along the spinline, up to 160 cm below the spinneret, is shown in Figure 3 for take-up velocities from 100 to 1000 m/min. Birefringence increases gradually with distance from the spinneret. At any particular position below the spinneret, the birefringence increases monotonically with take-up velocity or take-up stress.

Interpretation

The WAXS patterns for the fibers spun through air and through the humid chamber show a single diffuse halo. The patterns correspond to those of the amorphous quenched nylon 6 samples described by Roldan and Kaufman[14] and not to Ziabicki and Kedzierska's[13] patterns for as-spun fibers.

In order to properly interpret these patterns, we need to explore the variation of crystallization rates with respect to temperature. Studies of the crystallization kinetics of nylon 6 under quiescent conditions have been reported by Burnett and McDevit[45] and Magill,[46] among others. Magill finds a maximum in his rate data at 138°C, which is well above the temperatures (80–99°C) of the present fibers at the position of the WAXS measurements. These results indicate that any crystallization that would occur during the actual spinning process should already have taken place by the position of our measurements.

The reason for the failure of nylon 6 to crystallizate in the spinline is certainly

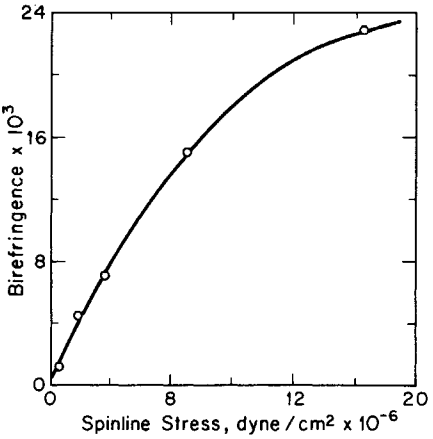

Fig. 7. Variation of fiber birefringence with spinline stress.

the slowness of the crystallization kinetics relative to the period which the melt spends in this temperature environment. As we have noted, studies of the crystallization kinetics of nylon 6 under quiescent conditions have been reported by Burnett and McDevit[45] and Magill.[46] If these are compared with similar experimental results on polyethylene[47] and polypropylene,[48] it is found that at equivalent amounts of supercooling below the melting piont, i.e., $T_m - T$, the crystallization rates are approximately an order of magnitude smaller for the nylon 6. The enhancement of the crystallization kinetics in the spinline by the presence of tension is not sufficient for nylon 6 to allow crystallization to occur under the spinning conditions for which we have performed on-line measurements (take-up velocities up to 1000 m/min and take-up stresses up to 38×10^6 dynes/cm^2, see our earlier paper[39]).

The relative behavior of nylon 6 and polyolefins in the spinline can be expressed in terms of the continuous cooling curves of our earlier papers.[35,36] This is shown in Figure 4. It must be realized that the curves in Figure 4 are schematic rather than actual in the present instance and are intended only to describe the situation qualitatively. In principle, we would expect different crystallization start curves for different spinning stresses. With increasing spinning stress, these curves would move to the left on the time axis to shorter times as a result of the increased crystallization kinetics. For nylon 6 spun under normal spinning conditions, the crystallization start curve lies at sufficiently large times and the rate of cooling of the filament from above the melting point is sufficiently rapid to prevent the cooling curve from intersecting the crystallization start curve and no crystallization is observed.

As indicated in Figure 4, this is not true for polyethylene and polypropylene, and these filaments crystallize during spnning. It is conceivable that spinning at higher take-up velocities (e.g., several thousand meters per minute) might increase the crystallization rates sufficiently to offset increases in cooling rates and allow nylon 6 to crystallize during spinning. Some indication that this may be the case is evidenced by the birefringence measurements as discussed below. Because of limitations in the operating speed of our take-up equipment and in the sensitivity of the x-ray technique for small-diameter filaments, we were unable to investigate this possibility fully.

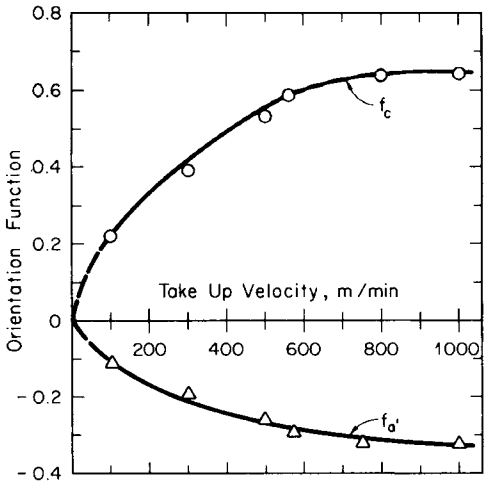

Fig. 8. Orientation factors for nylon 6 fiber as a function of take-up velocity.

Placing an isothermal column below the spinneret in which the temperature is equal to that at the maximum of the crystallization rate–temperature curve may well allow crystallization in the spinline. Such a procedure has been carried out by Ishibashi, Aoki, and Ishii[19] who report increases in fiber birefringence induced by the presence of such a chamber. This point is also illustrated in Figure 4.

The increase in birefringence with distance from the spinneret, Figure 3, can be interpreted as indicating increased molecular orientation with increased draw-down in the spinning filament. Increasing the take-up velocity at constant mass flow rate and spinneret dimensions causes an increase in the melt draw-down and cooling rate of the filament. This then results in greater molecular orientation and birefringence at a given distance from the spinneret.

At high take-up velocities, the birefringence continues to increase after the filament has reached its final diameter and velocity. This effect can be seen by comparing the birefringence profiles of Figure 3 with the velocity profiles presented as Figure 5 of our previous paper.[39] These data show, for example, that a volume element in the filament has reached the take-up velocity of 556 m/min at a point 100 cm from the spinneret. The data of Figure 3 clearly show the birefringence continuing to increase beyond this position. In this part of the spinline, the filament temperature is still above the glass transition temperature and molecular rearrangement in response to the high spinline stresses is possible. It is also possible that the increase in birefringence is due to incipient crystallization or paracrystalline order. However, the size of any such crystallite or ordered regions is too small to obtain any detectable crystalline interference effects on the on-line WAXS patterns.

AS-SPUN FIBERS

Results

Figure 5 shows WAXS patterns of spun fiber taken in a vacuum camera immediately after spinning. The time required to take the sample from the bobbin

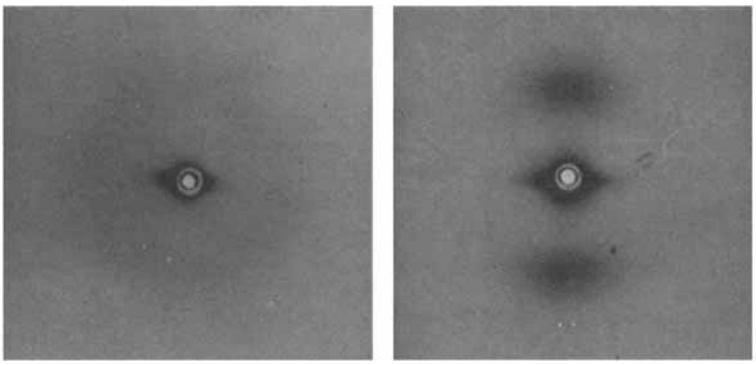

(a) (b)

Fig. 9. SAXS patterns for the equilibrated as-spun filaments: (a) 100 m/min; (b) 1000 m/min.

and put it in the vacuum camera was less than 5 min. It is seen that the sample spun at 200 m/min shows the same single diffuse ring as the on-line patterns. The sample spun at 1000 m/min shows a pattern with two readily observable but broadened reflections at d-spacings of 8.2 and 4.13 Å. The 8.2-Å spacing is meridional, and the 4.13-Å spacing is most intense at the equator though a complete faint ring may be observed.

After conditioning for 24 hr at 65% relative humidity and 24°C, the x-ray patterns of all the samples, including those spun at low take-up velocities, exhibited weak, broadened reflections at 8.2 and 4.13 Å spacings (Fig. 6).

The level of orientation of melt-spun fibers, either before or after conditioning, increased with take-up velocity and take-up stress (see Figs. 5, 6, and 7). Figure 7 shows the variation of conditioned fiber birefringence with spinline stress. In addition to the obvious increase of birefringence with spinline stress, it should be noted that the birefringence of the conditioned fibers is much greater than the maximum birefringence observed on the running spinline; compare Figure 6 with Figure 3.

The crystalline orientation of the spun and conditioned fibers was determined using an x-ray diffractometer as described in the experimental section. The values of orientation factors are shown in Figure 8 plotted as a function of the take-up velocity.

Typical SAXS patterns for conditioned filaments are shown in Figure 9. At low take-up velocities, a diffuse ring is observed. At higher take-up velocities, a "two-point" pattern develops. This again indicates an increase in orientation with take-up velocity. The long period spacing computed from the SAXS pattern did not vary appreciably with take-up velocity; it had a value of 64 ± 2 Å for take-up velocities from 100 to 2400 m/min.

Discussion

The WAXS patterns of Figure 5(b) and Figure 6 are similar to those of Ziabicki and Kedzierska.[13] They may be interpreted to mean that these samples have partially crystallized in a form having a pseudohexagonal unit cell. We will call this the γ form. We believe that it is similar to the pseudohexagonal, paracrystalline γ form described by Roldan and Kaufman[14] and consists of a poorly

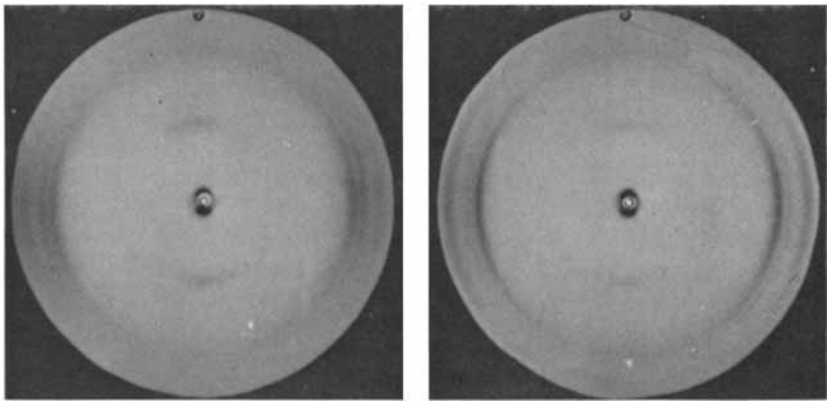

(a)

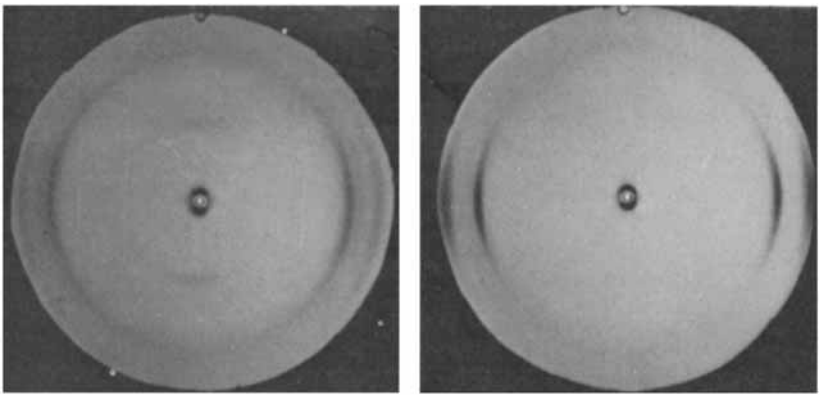

(b)

Fig. 10. WAXS patterns for nylon 6 fibers annealed in (a) water and (b) 20% formic acid at different temperatures.

developed version of their β form (hexagonal). This latter phase has also been called the γ form by several investigators.[8–11,15]

It is interesting that Figure 5(a) exhibits a diffuse halo which is essentially identical to that observed in the on-line x-ray patterns (d = 4.2 Å). Evidently, this sample, spun at a take-up velocity of only 200 m/min, did not crystallize into the γ form during the time required to put the sample in the vacuum camera and obtain the diffraction pattern. Under similar conditions, the sample spun at 1000 m/min exhibits a pattern [Fig. 5(b)] which is characteristic of a well-oriented γ form. This difference appears to be due to the higher rate of nucleation caused by higher molecular orientation in the latter sample. This higher molecular orientation was generated as a result of the higher spinline stress developed by the high take-up rate. Thus, although nylon 6 does not crystallize on the spinline, it does so on the bobbin, and the rate of this process depends on the molecular orientation developed by the spinning conditions.

After conditioning in a humid atmosphere, all of the spun filaments partially crystallized into the γ form. This increase in crystallinity has been observed by other investigators also and is attributed to the plasticizing action of water molecules which increase the chain mobility.

The process of conditioning also causes an increase in the molecular orientation

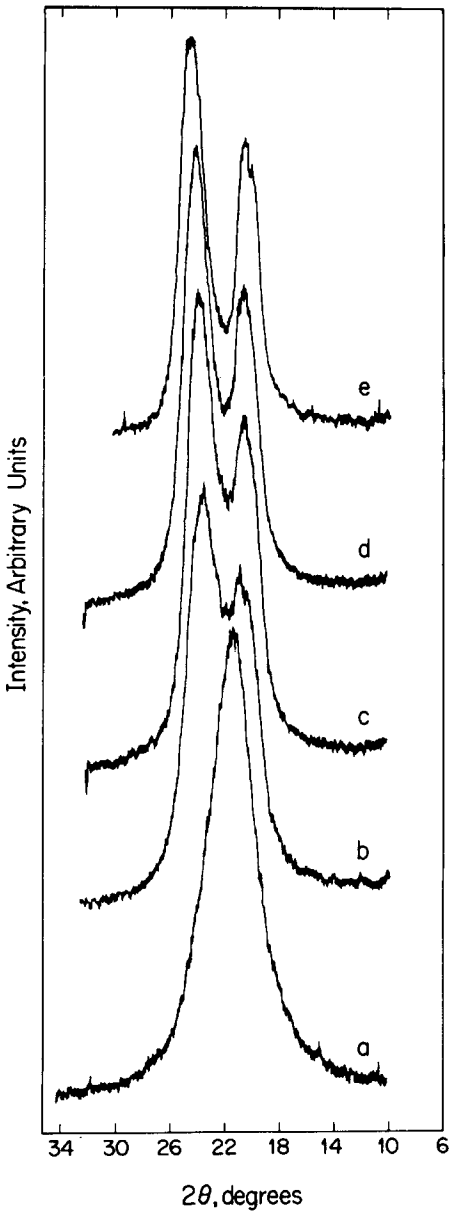

Fig. 11. Typical equatorial diffractometer scans for nylon 6 filaments. Samples spun at 556 m/min take-up velocity. The curves have been displaced along the ordinate for clarity: (a) as-spun and conditioned; (b) annealed 2 hr in water at 60°C; (c) annealed 2 hr in air (65% relative humidity) at 150°C; (d) annealed 2 hr in water at 100°C; (e) annealed 2 hr in 20% formic acid at 102°C.

of nylon 6 filaments. This is clear from a comparison of the birefringence after conditioning (Fig. 7) with the on-line values (Fig. 3). The birefringence of the conditioned filaments is of order 10 to 15 times greater than the maximum values measured on the spinline. The bulk of this change is evidently due to orientation induced by crystallization.

As shown in Figure 8, the c-axis crystalline orientation factor, f_c, increases with take-up velocity and spinline stress while $f_{a'}$ decreases. This, of course, indicates

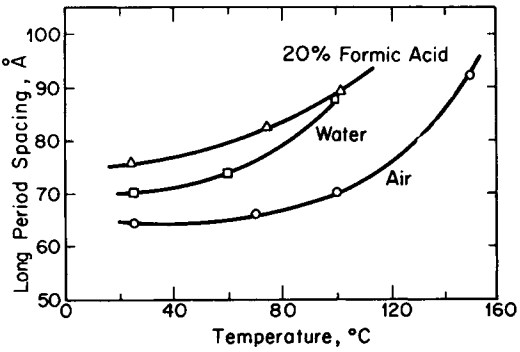

Fig. 12. Variation of long-period spacing with annealing treatment.

that the c axis or polymer chain direction tends to become more aligned with the fiber axis while the a'-direction becomes more nearly perpendicular to the fiber axis. This general behavior is very similar to that exhibited by several other polymers, including those that crystallize on the spinline such as polyethylene, polypropylene, and polyoxymethylene.[33,35,36]

In previous work on polyethylene,[33] orientation factors for each of the three crystallographic axes, f_a, f_b, and f_c, could be uniquely determined as a result of the orthorhombic symmetry of the polyethylene unit cell. This information, together with supporting information from SAXS and electron microscopy, prompted Dees and Spruiell[33] to suggest a detailed morphologic model for melt-spun polyethylene filaments based on the "row structure" models of Keller and Machin[49] (see also Spruiell and White[35,36]). According to this model, the morphology of polyethylene filaments changes from "spherulitic" at very low take-up velocities and spinline stresses to a "row nucleated" or "cylindritic" morphology at high take-up velocities and spinline stresses. In the latter case, ribbon-like lamellar crystals are assumed to grow radially outward in a direction perpendicular to the fiber axis. This results in an alternating texture of crystalline lamellae and interlamellar (disordered) regions along the fiber axis. This latter feature accounts for the observed two-point SAXS patterns of filaments spun at high take-up rates.

In the case of spun and conditioned nylon 6 filaments, the orientation data do not generally provide as much information as in the case of polyethylene. Because of the pseudohexagonal symmetry of the nylon 6 unit cell, we cannot distinguish between two axes in the plane perpendicular to the c-axis. The available data, including the SAXS patterns, are consistent with the general trend described above for the polyethylene filaments. The SAXS patterns of nylon 6 spun at low take-up velocity (~100 m/min) show a diffuse ring. This can be interpreted as indicative of an unoriented lamellar structure, probably a spherulitic morphology. The SAXS patterns of nylon 6 spun at high take-up velocities show a broadened, two-point diagram. This suggests lamellae growing perpendicular to the fiber axis and consisting of alternate crystalline and intercrystalline (amorphous) regions. In support of this suggestion, it may be noted that chain-folded lamellar crystals of nylon 6 have been produced by crystallization from solution.[50,51] Infrared studies on bulk-crystallized aliphatic polyamides also suggest the existence of a chain-folded structure.[52] Evidence for chain folding in nylon 66 has been discussed by Dismore and Statton.[53] A model

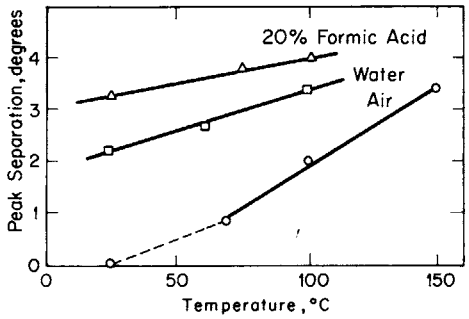

Fig. 13. Apparent angular separation between 200 and 002,202 reflections as a function of annealing treatment.

of chain-folded lamellar structure in the melt-spun and conditioned nylon 6 fibers thus seems reasonable.

The fact that the long periods of fibers spun over a wide range of take-up velocities were equal is not surprising in view of the fact that all the samples crystallized at a similar low temperature on the bobbin. The value of 64 Å may be compared with a value of 60 Å obtained by Geil[50] for single crystals of nylon 6. The observed long period corresponds to about four monomeric units. This value is very similar to that found by Dreyfuss and Keller[54] for nylons 66, 610, and 612 in lath-shaped products crystallized from solution.

ANNEALING TREATMENTS

Results

Annealing treatments were carried out in air, water, and 20% formic acid solution. The effects on the WAXS patterns of annealing spun filaments are illustrated in Figures 10 and 11. Annealing causes the intensity of the meridional reflection at 8.2 Å to decrease and the equatorial peak corresponding to 4.13 Å to divide into two reflections. This behavior is best shown using equatorial diffractometer scans as illustrated in Figure 11.

Annealing also produces changes in the long-period spacings obtained from SAXS. The long periods are shown as a function of annealing temperature in Figure 12 for samples annealed 2 hr in air, water, or 20% formic acid.

Interpretation

The WAXS patterns of Figures 10 and 11 indicate a transformation from the pseudohexagonal form to a monoclinic structure. The equatorial 100 reflection of the pseudohexagonal structure appears to split into two peaks which can be indexed as 200 and the doublet 002,202 of the monoclinic γ form. The peak positions and thus the d-spacings and unit cell constants of this form appear to vary with the annealing treatment. The most completely transformed samples, those annealed 2 hr in 20% formic at 102°C, have d-spacings which correspond closely to the monoclinic α form of Holmes, Bunn, and Smith.[6] The less completely transformed samples appear to correspond to what Roldan and Kaufman[14] called "paracrystalline α form."

The apparent angular separation of the 200 and 022,202 doublet was determined from diffractometer traces and is plotted in Figure 13 as a function of

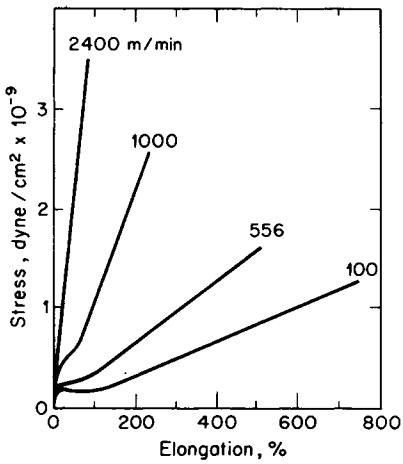

Fig. 14. Stress vs strain curves for as-spun nylon 6 fibers taken up at varying velocities.

annealing temperature and environment. This can be used as an indicator of the degree of transformation resulting from the annealing treatment. Clearly, the 20% formic acid solution is most effective in producing the transformation from the pseudohexagonal to the monoclinic α form. Of the three media investigated, the rate of transformation is slowest in air. For any of the three media, the rate of transformation increases with annealing temperature.

The reason for the difference in transformation rates in air, water, and 20% formic acid must involve the role of the medium in helping to temporarily break up hydrogen bonding; this presumably accommodates chain rearrangement, and the structure proceeds toward equilibrium more rapidly. Of the three media investigated, 20% formic acid is most effective in this regard, a point made clear by the fact that nylon 6 fibers dissolve in 90% formic acid, and this fluid may be used as a solvent for wet spinning.[30]

The long-period spacings were effected by both annealing temperature and environment. In general, samples which exhibited the greatest transformation to the α form also seemed to have the greatest long-period spacings. On annealing in air, the long-period spacing increased gradually with temperature. This behavior is similar to that observed for other polymer fibers such as polyethylene[55,56] and polypropylene,[57] but it seems to differ from the behavior of crystalline mats of aliphatic polyamides such as nylons 66, 610, and 612 grown from solution.[54]

MECHANICAL PROPERTIES

Results

Plots of engineering stress (force/initial cross-sectional area) as a function of elongation are shown in Figure 14 for fibers spun at different take-up velocities. The shapes of the "stress–strain" curves vary qualitatively as the take-up velocity or spinline stress changes. Increasing take-up rate results in an increasing tangent modulus, yield stress, and tensile strength, and decreasing elongation to break and natural draw ratio. The yield point seems even to disappear at high take-up velocities. In Figure 15, we plot the variation in tangent modulus, tensile strength, and elongation to break with take-up velocity.

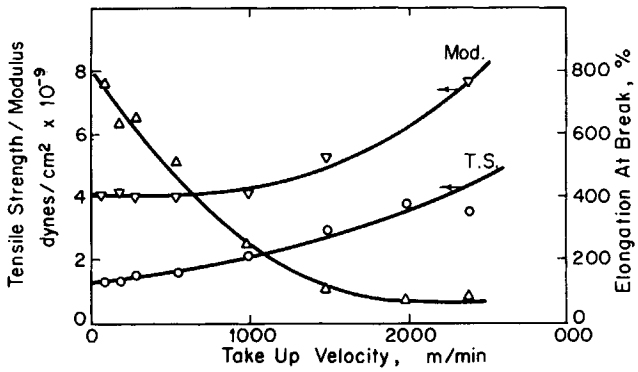

Fig. 15. Tangent modulus, tensile strength, and elongation to break as a function of take-up velocity.

Discussion

The variation of mechanical properties with spinning conditions results from variations in the morphology of the spun fibers. One of the major aspects of this morphology is the molecular orientation developed in the filament. In Figure 16, we plot the variations in the properties of Figure 15 with birefringence and with the c-axis crystalline (Hermans) orientation factor. Modulus and tensile strength increase with orientation and elongation to break decreases. The properties vary in a nonlinear way with either birefringence, which measures the average orientation in the sample, or with c-axis crystalline orientation factor. It is interesting that there is little change in modulus and tensile strength in the low orientation range, but these properties rise significantly at higher orientation levels. The behavior of the elongation to break appears just the opposite; its value seems more sensitive to orientation in the low orientation range. Either birefringence or c-axis crystalline orientation factor seems to give reasonable correlations of the mechanical properties. Similar correlations have been used by Abbott and White[37] and others[33–36,38] from our laboratories for polyethylene[33,36–38] and polypropylene.[34–36]

CONCLUSIONS

1. Nylon 6 filaments melt spun through ordinary air or air saturated with moisture do not crystallize in the spinline at take-up rates below 1500 m/min. The present experiments were inconclusive for filaments spun at higher rates.
2. Nylon 6 filaments "crystallize" on the take-up bobbin into a paracrystalline pseudohexagonal structure. The rate of "crystallization" and the orientation in the filaments increase with take-up velocity and take-up stress. Orientation factors may be defined and measured to interpret this latter behavior.
3. The oriented, conditioned fibers exhibit a broadened two-point SAXS pattern which suggests the existence of a poorly developed row structure.
4. Annealing treatment with hot water or formic acid solutions transforms the pseudohexagonal structure to monoclinic. The rate of transformation increases with temperature and is greatest in acid solutions.
5. The stress–strain curves for as-spun fibers show increasing modulus and tensile strength and decreasing elongation to break with increasing take-up velocity and stress.

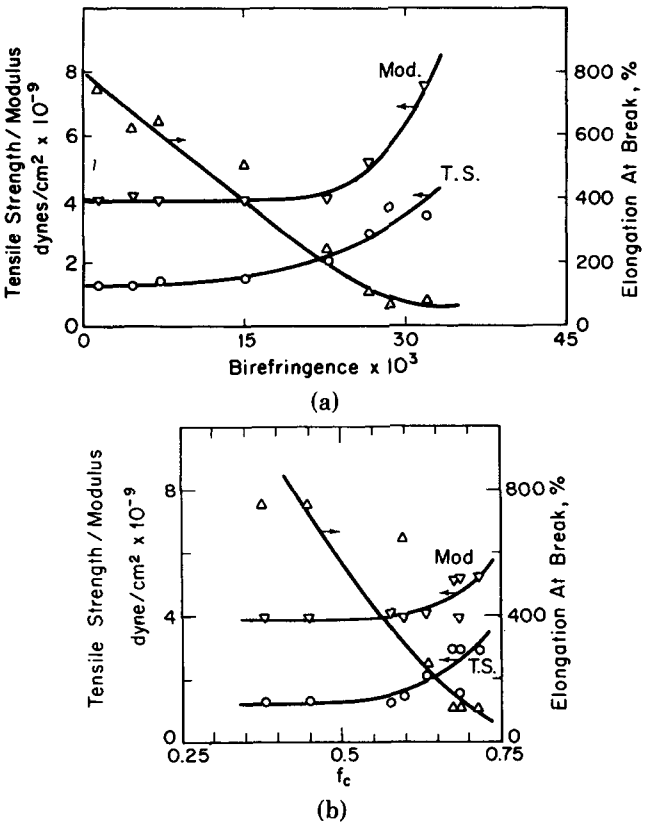

Fig. 16. Tangent modulus, tensile strength, and elongation to break as a function of (a) birefringence and (b) c-axis crystalline orientation factor f_c.

The authors would like to thank E. S. Clark, T. Ishibashi, M. Matsui, J. Parker, D. Prevorsek, and A. Rickards for helpful discussions on aspects of this research. This research was supported in part by the National Science Foundation.

References

1. W. Sbroli, in *Man-Made Fibers,* Vol. 2, H. Mark, S. Atlas, and E. Cernia, Eds., Wiley, New York, 1967.
2. W. H. Carothers and G. J. Berchet, *J. Amer. Chem. Soc.*, **52,** 5289 (1930).
3. W. H. Carothers and J. W. Hill, *J. Amer. Chem. Soc.*, **54,** 1566, 1579 (1932).
4. P. Schlack, Germ. Pat. 748,253 (1938); U.S. Pat. 2,241,321 (1941).
5. R. Brill, *Z. Phys. Chem.*, **B53,** 61 (1942).
6. D. R. Holmes, C. W. Bunn, and D. J. Smith, *J. Polym. Sci.*, **17,** 159 (1955).
7. S. Ueda and T. Kimura, *Chem. High Polym. Jpn.*, **15,** 243 (1958).
8. M. Tsuruda, H. Arimoto, and M. Ishibashi, *Chem. High Polym. Jpn.*, **15,** 619 (1958).
9. Y. Kinoshita, *Makromol. Chem.*, **33,** 1 (1959).
10. D. C. Vogelsong, *J. Polym. Sci.*, **1,** 1655 (1963).
11. K. Miyasaka and K. Ishikawa, *J. Polym. Sci. A-2,* **6,** 1317 (1968).
12. I. Sandeman and A. Keller, *J. Polym. Sci.*, **19,** 401 (1956).
13. A. Ziabicki and K. Kedzierska, *J. Appl. Polym. Sci.*, **2,** 14 (1959).
14. L. G. Roldan and H. S. Kaufman, *J. Polym. Sci., Polym. Lett. Ed.*, **B1** 603 (1963); L. G. Roldan, F. Rahl, and A. R. Patterson, *J. Polym. Sci.*, **C8,** 145 (1965).
15. J. Parker and P. H. Lindenmeyer, paper presented at the Fiber Society Meeting, Williamsburgh, Virginia, May 1974.
16. A. Ziabicki and K. Kedzierska, *J. Appl. Polym. Sci.*, **6,** 111 (1962).

17. I. Hamana, M. Matsui, and S. Kato, *Melliand Textilber.*, **4,** 382 (1969).
18. T. Ishibashi, K. Aoki, and T. Ishii, *J. Appl. Polym. Sci.*, **14,** 1597 (1970).
19. T. Ishibashi and T. Ishii, *J. Appl. Polym. Sci.*, **20,** 335 (1976).
20. W. M. Pasika, A. C. West, and E. L. Thurston, *J. Polym. Sci., Polym. Phys.*, **10,** 2313 (1972).
21. K. Sakaoku, N. Morosoff, and A. Peterlin, *J. Polym. Sci., Polym. Phys.*, **11,** 31 (1973).
22. A. Wasiak and A. Ziabicki, in *Fiber and Yarn Processing,* J. L. White, Ed., *Appl. Polym. Symp.*, **27,** 111 (1975).
23. H. Yumoto, *Bull. Chem. Soc. Jpn.*, **29,** 45 (1956).
24. H. Yumoto, *Bull. Chem. Soc. Jpn.*, **29,** 141 (1956).
25. H. Hattori, Y. Takagi, and T. Kawaguchi, *Bull. Chem. Soc. Jpn.*, **35,** 1163 (1962).
26. H. Hattori and Y. Takagi, *Bull. Chem. Soc. Jpn.*, **36,** 675 (1963).
27. T. Kitao, Ph.D. Dissertation, Kyoto University, 1975.
28. T. Kitao, H. Kobayoshi, S. Ikejami, and S. Ohya, *J. Polym. Sci., Polym. Chem.*, **11,** 2633 (1973).
29. T. Kiyotosukuri, H. Hasegawa, and R. Imamura, *Sen-i-Gakkaishi,* **26,** 399 (1970).
30. T. Hancock, J. E. Spruiell, and J. L. White, *J. Appl. Polym. Sci.*, **21,** 1227 (1977).
31. F. P. Chapell, M. F. Culpin, R. G. Gosden, and T. C. Tranter, *J. Appl. Chem.*, **14,** 12 (1964).
32. K. Katayama, T. Amano, and K. Nakamura, *Kolloid Z.-Z. Polym.*, **226,** 125 (1968).
33. J. R. Dees and J. E. Spruiell, *J. Appl. Polym. Sci.*, **18,** 1053 (1974).
34. H. Henson and J. E. Spruiell, unpublished research.
35. J. E. Spruiell and J. L. White, *Polym. Eng. Sci.*, **15,** 660 (1975).
36. J. E. Spruiell and J. L. White, in *Fiber and Yarn Processing,* J. L. White, Ed., *Appl. Poly. Symp.*, **27,** 121 (1975).
37. L. E. Abbott and J. L. White, in *U.S.–Japan Seminar on Polymer Processing and Rheology,* D. C. Bogue, M. Yamamoto, and J. L. White, Eds., *Appl. Polym. Symp.*, **20,** 247 (1973).
38. J. L. White, K. C. Dharod, and J. L. White, *J. Appl. Polym. Sci.*, **18,** 2539 (1974).
39. V. Bankar, J. E. Spruiell, and J. L. White, *J. Appl. Poly. Sci.*, **21,** 2135 (1977).
40. V. Bankar, Ph.D. Dissertation in Chemical Engineering, The University of Tennessee, Knoxville, 1976.
41. J. J. Hermans, P. H. Hermans, D. Vermaas, and A. Weidinger, *Rec. Trav. Chim.*, **65,** 427 (1946).
42. R. S. Stein, *J. Polym. Sci.*, **31,** 327 (1958).
43. Z. W. Wilchinsky, *J. Appl. Phys.*, **30,** 792 (1959); *ibid.*, **31,** 1969 (1960); *Advan. X-Ray Anal.*, **6,** 231 (1962).
44. T. Kitao, S. Ohya, J. Furukawa, and S. Yamashita, *J. Polym. Sci., Poly. Phys.*, **11,** 1091 (1973).
45. B. B. Burnett and W. F. McDevit, *J. Appl. Phys.*, **28,** 1101 (1957).
46. J. H. Magill, *Polymer,* **3,** 655 (1962).
47. L. Mandelkern, in *Growth and Perfection of Crystals,* R. H. Doremus, B. W. Roberts, and D. Turnbull, Eds., Wiley, New York, 1958, p. 478.
48. J. H. Griffith and B. G. Ranby, *J. Polym. Sci.*, **38,** 107 (1959).
49. A. Keller, and M. Machin, *J. Macromol. Sci.-Phys.*, **81,** 41 (1967).
50. P. H. Geil, *J. Polym. Sci.*, **44,** 449 (1960).
51. M. Ogawa, T. Ota, O. Yoshizaki, and E. Nagai, *Polym. Lett.*, **1,** 57 (1963).
52. J. L. Koenig and M. C. Agboatwala, *J. Macromol. Sci.*, **B2,** 391 (1968).
53. P. F. Dismore and W. O. Statton, *J. Polym. Sci.*, **C13,** 133 (1966).
54. P. Dreyfuss and A. Keller, *J. Macromol. Sci.*, **B4**(4), 811 (1970).
55. W. O. Statton and P. H. Geil, *J. Appl. Polym. Sci.*, **3,** 357 (1960).
56. R. Corneliussen and A. Peterlin, *Makromol. Chem.*, **105,** 193 (1967).
57. H. D. Noether and W. Whitney, *Kolloid Z.-Z. Polym.*, **251,** 991 (1973).

Received July 16, 1976